Supplementary Information

Promoting optoelectronic properties of $Cs_2AgBiBr_6$ nanocrystals by formation of heterostructures with BiOCl nanosheets

Lei Yang, Yuping Li, Wei Zhang, Yanlei Liu, Jiacheng Cao, Yang Cao, Jusheng Bao, Zhiwei Wang,* Lin Wang* and Xiao Huang*

Experimental Section

Materials: $Bi(NO_3)_3 \cdot 5H_2O$ (bismuth nitrate pentahydrate, ≥ 98%, Sigma-Aldrich, America), PVP (polyvinyl pyrrolidone, K13-18, Mackin, China), D-mannitol ($C_6H_{14}O_6$, 99%, Alfa Aesar, England), NaCl (sodium chloride, ≥ 99.9 %, Shanghai Chemical Reagent Co., Ltd., China), AgBr (silver bromide, ≥ 99.9 %, Aladdin, China), $BiBr_3$ (bismuth tribromide, ≥ 98%, Sigma-Aldrich, America), Cs_2CO_3 (cesium carbonate, ≥ 99.9 %, Aladdin, China), 1-octadecene (ODE, 90%, Sigma-Aldrich, America), OA (oleic acid, 85%, TCI, Japan), OLA (oleylamine, 90%, Sigma-Aldrich, America), toluene (≥ 99.9%, Merck Millipore, Germany), chloroform (≥ 99%, Shanghai Chemical Reagent Co., Ltd., China), hexane (≥ 98%, Shanghai Chemical Reagent Co., Ltd., China), ethanol (≥ 99.5%, Shanghai Chemical Reagent Co., Ltd., China). All reagents were used as received without any purification.

Synthesis of BiOCl nanosheets: Typically, 227 mg mannitol and 200 mg PVP were dissolved in 12.5 mL of deionized water under vigorous stirring for 10 min, followed by the addition of 243 mg $Bi(NO_3)_3 \cdot 5H_2O$. Into the mixture, 2.5 mL of saturated NaCl aqueous solution (0.1 M) was added dropwise. After stirring for 20 min, the final solution was transferred to a Teflon-lined stainless-steel autoclave (20 mL) and heated at 160 °C for 3 h. After cooling down to room temperature naturally, the obtained precipitate was centrifuged at 7000 rpm and washed several times with water and ethanol, and finally re-dispersed in 5 mL ethanol as a stock solution for further use.

Preparation of Cs-oleate precursor: Typically, 407 mg Cs_2CO_3 and 1.5 mL OA were

mixed with 20 mL ODE in a 100 mL three-neck flask. This mixture was degassed at 120 °C under vacuum for 30 min, and then heated to 150 °C in Ar gas until a clear solution was formed. The Cs-oleate precursor solution was stored under an Ar atmosphere for further use.

Synthesis of CABB nanocrystals: In a typical reaction, 90 mg $BiBr_3$, 20 mg AgBr, and 5 mL ODE were mixed in a 100 mL three-necked flask and heated to 110 °C for 15 min under vacuum. 1.0 mL of OA and 0.5 mL of OLA were heated to 70 °C separately before being added to the reaction flask. The reaction temperature was then raised to 200 °C under an Ar atmosphere before 0.8 mL of Cs-oleate solution pre-heated at 110 °C was injected rapidly into the flask under vigorous stirring. The color of the solution changed from yellow to orange rapidly. Three minutes later, the heating was stopped and the flask was cooled in an ice-water bath. The final product was washed with hexane by centrifugation at 10000 rpm for three times, and finally re-dispersed in 5 mL hexane as a stock solution for further use.

Synthesis of CABB/BiOCl heterostructures: In a typical reaction, 90 mg $BiBr_3$, 20 mg AgBr, and 5 mL ODE were mixed in a 100 mL three-necked flask and heated to 110 °C for 15 min under vacuum. 1.0 mL of OA and 0.5 mL of OLA were heated to 70 °C separately before being added to the reaction flask. At the same time, 0.5 ml of BiOCl nanosheet stock solution was washed three times with toluene and finally re-dispersed in 5 mL toluene before being added to the reaction flask. The reaction temperature was then raised to 200 °C under an Ar atmosphere before 0.8 mL of Cs-oleate solution pre-heated at 110 °C was injected rapidly into the flask under vigorous stirring. The heating was stopped after 3 min and the flask was cooled in an ice-water bath. The final product was washed with chloroform by centrifugation at 8000 rpm for three times, and finally re-dispersed in 2 mL hexane as a stock solution for further use.

Characterizations: The morphological and structural characterizations of the products were conducted with TEM operated at 200 kV (JEOL 2100 Plus and JEOL 2100F, Japan) and XRD (SmartLab Rigaku, Japan, with Cu Kα radiation at λ = 1.54 Å). The absorption spectra of the materials were measured on a UV-vis spectrophotometer (UV-1750, Shimadzu, Japan). Excitation spectra of the materials were obtained using an F4600 fluorescence spectrometer (Hitachi, Japan). PL spectra of the sample films were measured using the Finder Smart confocal Raman system (Zolix FST2-MPL501-405C1) with a 405 nm laser. The lifetime and low-temperature time-correlated single-photon

counting spectra of sample films placed in a vacuum cryostat were measured on a fluorescence spectrophotometer (Edinburgh Instruments, England) under a 375 nm microsecond xenon lamp (Edinburgh Instruments, England). The valence bands of the products were measured with an X-ray photoelectron spectroscopy (XPS, PHI 5000 VersaProbe, Japan). Au interdigitated electrodes with a 10 μm gap (Mecart Sensor Tech. Co., Ltd., China) were used for the photoresponse measurements. 1 μL of the prepared products was drop-cast onto the electrodes. I-V and I-t curves of the device were measured on a semiconductor characterization system (Keithley 4200, USA) at room temperature. The laser power intensity was measured and calibrated by a power meter (LP1, Sanwa Electric Instrument Co., Ltd., Japan).

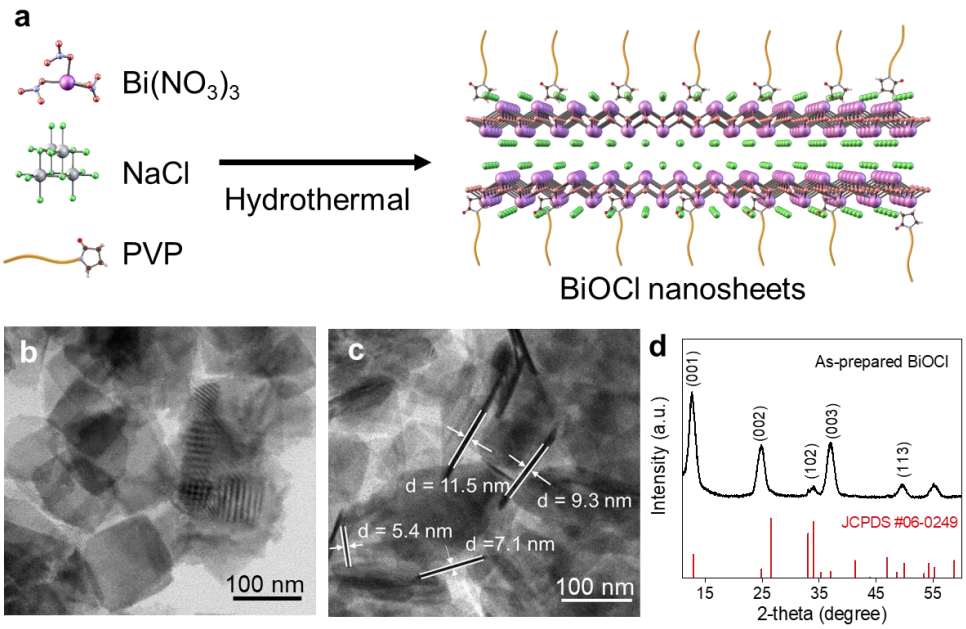

Figure S1 (a) Schematic illustration of the hydrothermal synthesis of BiOCl nanosheets. (b, c) TEM images and (d) XRD pattern of BiOCl nanosheets.

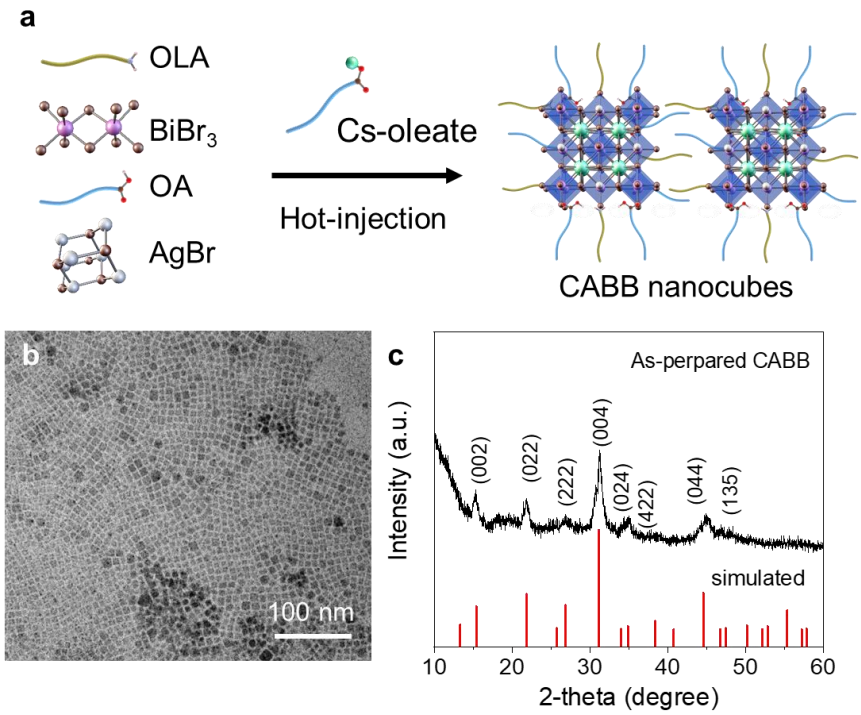

Figure S2 (a) Schematic illustration of the synthesis of CABB nanocrystals. (b) TEM image and (c) XRD pattern of CABB nanocrystals.

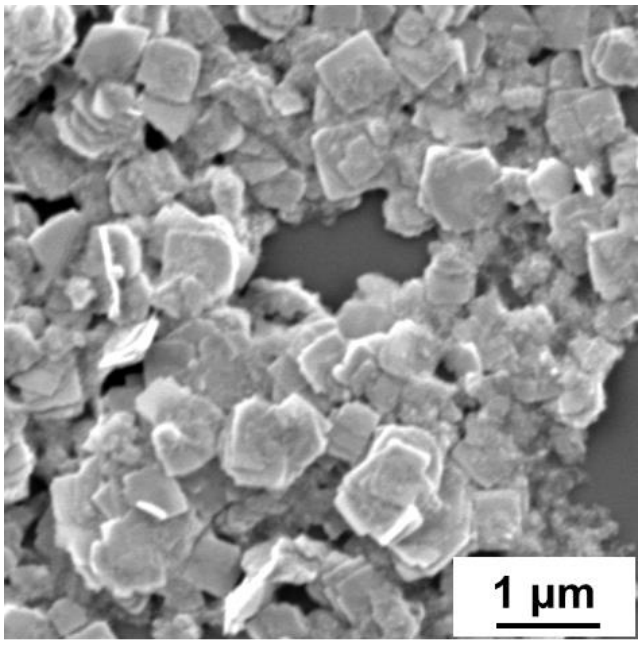

Figure S3. SEM image of CABB/BiOCl heterostructures.

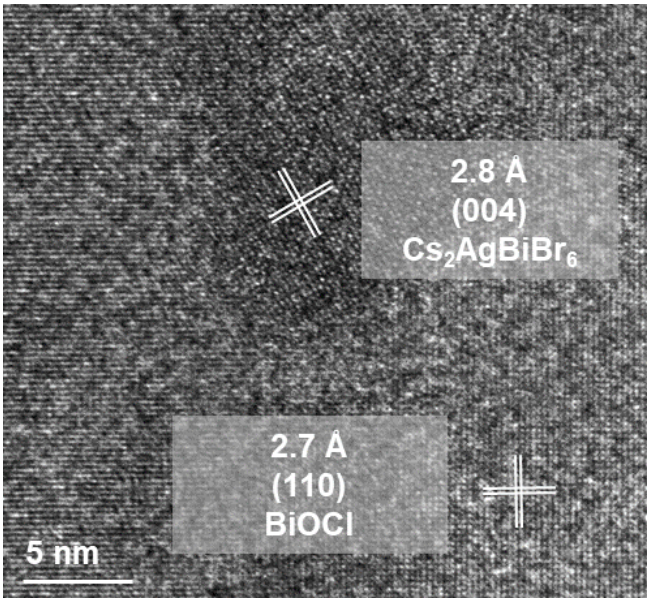

Figure S4 HRTEM image of a CABB/BiOCl heterostructure.

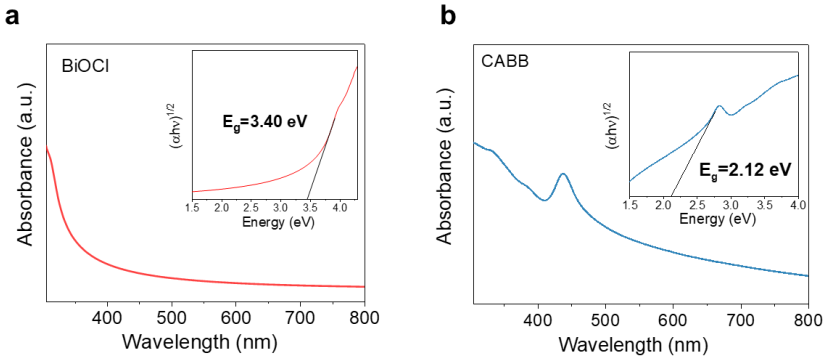

Figure S5 UV-vis spectra at room temperature and plots of $(\alpha h\nu)^{1/2}$ versus photon energy ($h\nu$) of (a) BiOCl and (b) CABB.

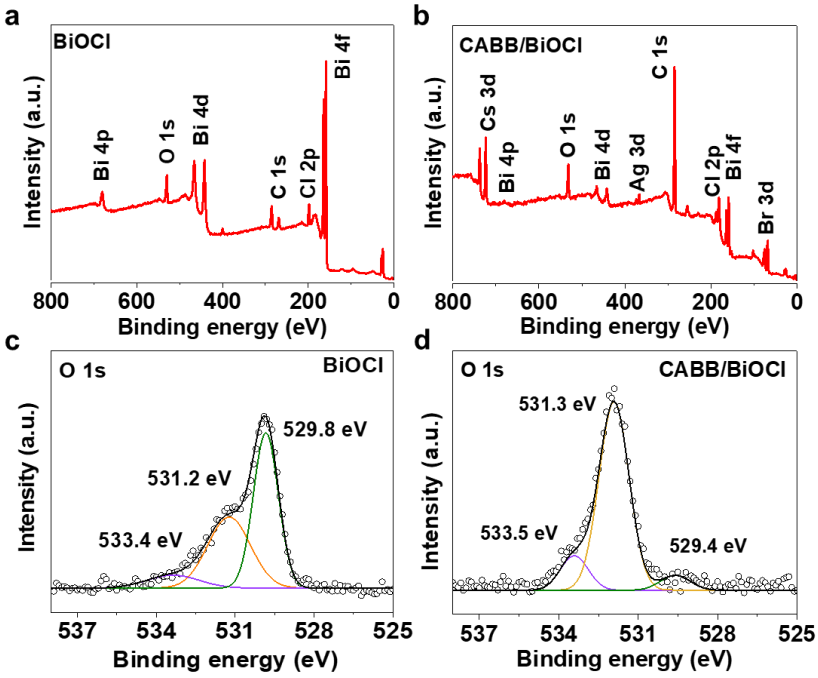

Figure S6 XPS survey spectra of (a) BiOCl nanosheets and (b) CABB/BiOCl heterostructures. High-resolution O1s spectra of (a) BiOCl nanosheets and (b) CABB/BiOCl heterostructures. The binding energies at ~533, 531 and 529 eV could be attributed to oxygen vacancies,[1] chemisorbed oxygen,[2] and oxygen in the lattice of BiOCl,[3] respectively.

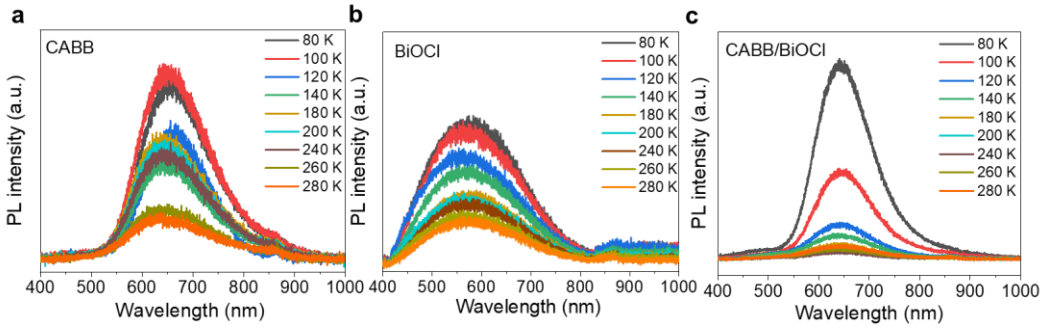

Figure S7 Temperature dependent PL spectra of (a) CABB nanocrystals, (b) BiOCl nanosheets, and (c) CABB/BiOCl heterostructures. The laser power density was 1 μw/cm^2.

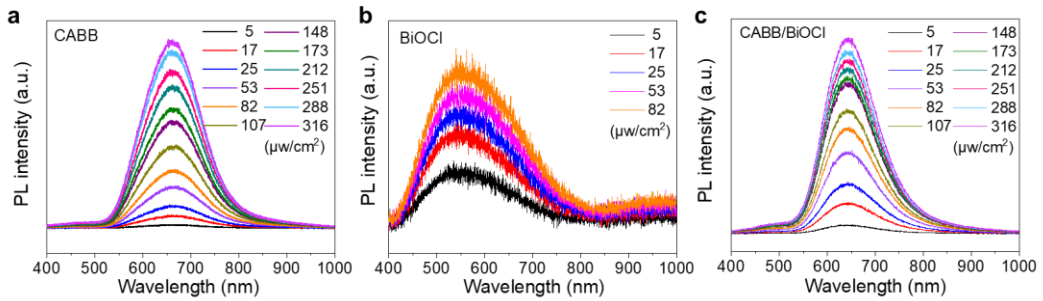

Figure S8 Laser power dependent PL spectra of (a) CABB nanocrystals, (b) BiOCl nanosheets and (c) CABB/BiOCl heterostructures at 80 K. The excitation wavelength was 405 nm.

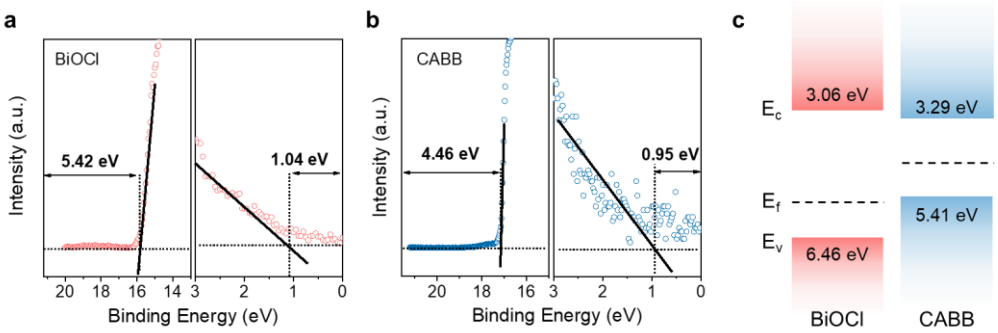

Figure S9 Zoomed-in UPS spectra showing the positions of the Fermi levels relative to the vacuum (set to 0) and the positions of the VBM relative to the Fermi level for (a) BiOCl nanosheets and (b) CABB nanocrystals. (c) Schematic of the band level diagram of BiOCl and CABB at room temperature.

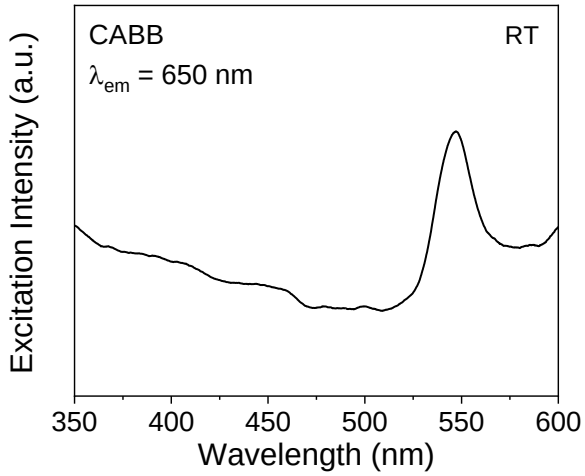

Figure S10 Excitation spectrum of CABB at an emission wavelength of 650 nm.

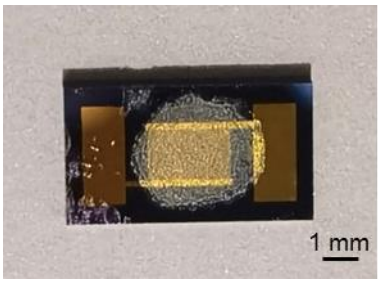

Figure S11 Optical image of a photodetector device.

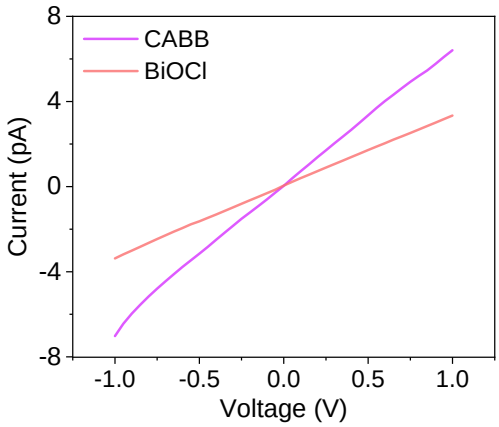

Figure S12 I-V curves of CABB and BiOCl in dark under a bias voltage of 1 V.

References

1. X. Wang, X. Liu, G. Liu, C. Zhang, G. Liu, S. Xu, P. Cui and D. Li, *Catal. Commun.*, **2019**, 130, 105769.

2. H. Chen, A. Sayari, A. Adnot and F. ç. Larachi, *Appl. Catal. B*, **2001**, 32, 195-204.

3. L. Zhang, W. Wang, D. Jiang, E. Gao and S. Sun, *Nano Res.*, **2014**, 8, 821-831.